p K a Calculations of Aliphatic Amines, Diamines, and Aminoamides via Density Functional Theory with a Poisson−Boltzmann Continuum Solvent Model

ARTICLE *in* THE JOURNAL OF PHYSICAL CHEMISTRY A · JUNE 2007

Impact Factor: 2.69 · DOI: 10.1021/jp071040t · Source: PubMed

3 AUTHORS:

Vyacheslav S Bryantsev
Oak Ridge National Laboratory
77 PUBLICATIONS **2,245** CITATIONS
SEE PROFILE

Mamadou Diallo
KAIST and Caltech
48 PUBLICATIONS **2,071** CITATIONS
SEE PROFILE

William A. Goddard
California Institute of Technology
1,345 PUBLICATIONS **68,479** CITATIONS
SEE PROFILE

pK_a Calculations of Aliphatic Amines, Diamines, and Aminoamides via Density Functional Theory with a Poisson−Boltzmann Continuum Solvent Model

Vyacheslav S. Bryantsev,[†] Mamadou S. Diallo,*[,†,‡] and William A. Goddard, III*[,†]

Materials and Process Simulation Center, Beckman Institute 139-74, California Institute of Technology, Pasadena, California 91125, and Department of Civil Engineering, Howard University, Washington, DC 20059

Received: February 6, 2007; In Final Form: March 14, 2007

In order to make reliable predictions of the acid−base properties of macroligands with a large number of ionizable sites such as dendrimers, one needs to develop and validate computational methods that accurately estimate the acidity constants (pK_a) of their chemical building blocks. In this article, we couple density functional theory (B3LYP) with a Poisson−Boltzmann continuum solvent model to calculate the aqueous pK_a of aliphatic amines, diamines, and aminoamides, which are building blocks for several classes of dendrimers. No empirical correction terms were employed in the calculations except for the free energy of solvation of the proton (H^+) adjusted to give the best match with experimental data. The use of solution-phase optimized geometries gives calculated pK_a values in excellent agreement with experimental measurements. The mean absolute error is <0.5 pK_a unit in all cases. Conversely, calculations for diamines and aminoamides based on gas-phase geometries lead to a mean absolute error >0.5 pK_a unit compared to experimental measurements. We find that geometry optimization in solution is essential for making accurate pK_a predictions for systems possessing intramolecular hydrogen bonds.

1. Introduction

Amino and amido functionalized organic compounds are ubiquitous in nature. Their biological importance[1] has led to extensive studies of their structural and physicochemical properties. In addition to their relevance in biochemistry and pharmaceutical chemistry, amines and amides are attractive building blocks in supramolecular chemistry.[2] Depending on solution pH, amine-based ligands can act as both cation and anion chelators.[3] Amide-containing receptors also exhibit dual cation/anion binding properties. They have emerged as attractive building blocks for a variety of anion receptors due to their relatively strong hydrogen bond donor N−H groups.[3] In addition, they contain oxygen and nitrogen heteroatoms that can coordinate with metal ions.[4]

We are interested in the proton-, cation-, and anion-binding properties of diamines and aminoamides as building blocks for macroligands of well-defined molecular size, shape, and composition such as dendrimers.[5] Examples of industrially important poly(propylenimine) (PPI) and poly(amidoamine) (PAMAM) dendrimers with amine and amidoamide functional groups are shown in Figure 1. The structures and anion/cation binding properties of PAMAM and PPI dendrimers in aqueous solutions and at solid−water interfaces strongly depend on solution pH, that is, their acid−base properties. A major focus of our current research program on dendrimer nanotechnology is to develop and validate a multiscale modeling approach for predicting proton, anion, and cation binding to dendrimers in aqueous solutions. A key step toward this goal is the ability to accurately calculate acidity constants (pK_a) for small fragments of a dendrimer. In this article, we address this issue in some detail. The effect of the macroligand field (i.e., dendrimer matrix) on the acid−base properties of dendrimer fragments will be the subject of future studies.

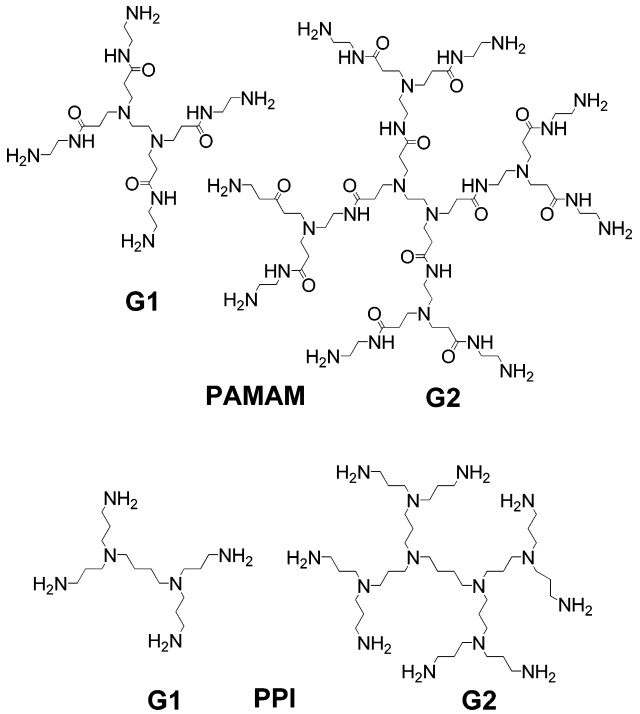

Figure 1. 2-D structures of the first (G1) and second (G2) generation of PAMAM and PPI dendrimers with terminal NH_2 groups.

Many reports have appeared in the literature describing computational methods of pK_a calculations (see, for example, refs 6−10). The most commonly used schemes couple quantum chemical calculations of gas-phase deprotonation energy with

* Authors to whom correspondence should be addressed. Beckman Institute MC 139-74, California Institute of Technology, Pasadena, CA 91125. Phone: 626 395 2730. Fax: 626 585 0918. E-mail addresses: wag@wag.caltech.edu (Goddard), and diallo@wag.caltech.edu (Diallo).
† California Institute of Technology.
‡ Howard University.

10.1021/jp071040t CCC: $37.00
Published on Web 05/01/2007

1	$MeNH_2$	**2**	$EtNH_2$
3	$PrNH_2$	**4**	*iso*-$PrNH_2$
5	*tert*-$BuNH_2$	**6**	$(Me)_2NH$
7	$(Et)_2NH$	**8**	$(Pr)_2NH$
9	$(Me)_3N$	**10**	$(Et)_3N$
11	$NH_2(CH_2)_2NH_2$	**12**	$NH_2(CH_2)_3NH_2$
13	$NH_2(CH_2)_4NH_2$	**14**	$MeNH(CH_2)_2NHMe$
15	$(Me)_2N(CH_2)_2N(Me)_2$	**16**	$(Me)_2N(CH_2)_3N(Me)_2$
17	$(Me)_2N(CH_2)_2N(Me)_2$	**18**	$NH_2CH_2CONH_2$
19	$MeNHCH_2CONH_2$	**20**	$MeNHCH_2CONHMe$
21	$MeNHCH_2CON(Me)_2$	**22**	$NH_2(CH_2)_2NHCOMe$
23	$(Me)_2N(CH_2)_2CONH_2$		

Figure 2. Amino-containing compounds studied in this work.

continuum dielectric models to account for solvent effects. However, continuum dielectric solvent models are often not adequate when dealing with solutes that have concentrated charge density with strong local solute−solvent interactions (e.g., ions). In these cases, it is critical to add explicit solvent molecules to the continuum solvent model system.[7] The accurate prediction of acidity constants is a challenging task. Differences of ∼1 pK_a unit between calculated and measured acidity constants are not uncommon. Because of this, several groups[8,9] have developed empirical correction terms for their calculated "raw" pK_a to improve agreement with measurements. For example, the pK_a module of the ab initio quantum chemistry software *Jaguar*[9] achieves an average accuracy of ∼0.5 pK_a unit using three empirical parameters for each functional group (the radius of the ion and two linear regression coefficients between calculated and measured pK_a). Recent studies of Liptak et al.[6g,6h] and others[6k] have described pK_a calculation protocols with no empirical correction factors based on highly accurate complete basis set (CBS) or Gaussian-n gas-phase methods with the CPCM continuum solvent model. However, pK_a calculations using these methods are not routinely feasible for medium and large molecules. The coupling of density functional theory (DFT) with a continuum solvent model has been shown[10] to provide a computationally viable and accurate pK_a calculation method.

Only a few studies of pK_a calculations for amines have been reported. The pioneering study of Tomasi et al.[6b] coupled ab initio quantum chemistry [MP4(SDTQ)/6-31G* level of theory] with an electrostatic polarizable continuum model to reproduce the experimentally observed order of basicities for methylamines. Kallies at al.[6d] used the SCI−PCM solvation model and DFT (B3LYP/6-31G* and B3LYP/aug-cc-pVDZ//B3LYP/6-31G* level of theory) to calculate the pK_a of selected aliphatic, alicyclic, and aromatic amines. Using empirical correction factors, they were able to obtain calculated pK_a values within 0.7 units of the measured values. However, the results of the calculations were less satisfactory when additional functional groups (e.g., hydroxyl, cyano, and methoxy) were present in the molecules. Only a few quantum chemical pK_a calculations for alkyldiamines have been reported.[8a,9b] To the best of our knowledge, no quantum chemical calculations of the second acidity constants (pK_{a2}) for diamines and aminoamides have been published in the literature except for the calculations on 2-aminoacetamide listed in ref 9b.

As a first step toward the determination of the pK_a of the amino and aminoamide groups of a dendritic macroligand, we coupled DFT with a Poisson−Boltzmann (PB) continuum solvation model to calculate the pK_a of aliphatic amines (**1**−**10**), diamines (**11**−**17**), and aminoamides (**18**−**23**) (Figure 2). Because aliphatic diamines and aminoamides are flexible, we carried out a detailed conformational analysis of these molecules. In all cases, the lowest-energy conformers were identified and used in subsequent pK_a calculations. No empirical correction terms were employed in these calculations. The use of solution-phase optimized geometries yields a perfect agreement between calculations and measurements with a mean absolute error <0.5 pK_a unit. Conversely, pK_a calculations for diamines and aminoamides based on gas-phase geometries lead to mean absolute error >0.5 pKa unit compared to experimental measurements. We find that geometry optimization in solution is essential for making accurate pK_a predictions for systems possessing intramolecular hydrogen bonds.

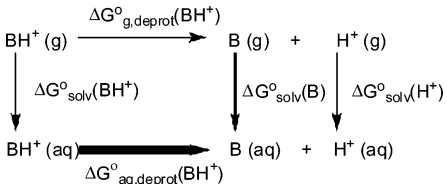

Figure 3. Thermodynamic cycle used in the calculation of pK_a.

2. Computational Methods and Procedures

2.1. pK_a Calculations. Acidity constants (pK_a) were calculated using the thermodynamic cycle[6a,6g] shown in Figure 3. In this cycle, $\Delta G°_{g,deprot}(BH^+)$ and $\Delta G°_{aq,deprot}(BH^+)$ are, respectively, the gas-phase and aqueous-phase standard free energy of deprotonation. $\Delta G°_{solv}(BH^+)$, $\Delta G°_{solv}(B)$, and $\Delta G°_{solv}(H^+)$ are the standard free energies of solvation for BH^+, B, and H^+, respectively. By definition, pK_a is given by

$$pK_a = -\log K_a = \Delta G°_{aq,\,deprot}(BH^+)/(2.303RT) \quad (1)$$

Note that all experimental and calculated gas-phase free energies are defined using an ideal gas at a pressure of 1 atm as the standard state ($\Delta G°_g$). Conversely, most tabulations of experimental and calculated free energies of solvation are defined as a transfer of a solute from its 1 M gas-phase state into its 1 M solution-phase state ($\Delta G*_{solv}$).[11,12] Thus, in order to combine gas-phase standard free energies of formation with standard free energies of solvation defined above, a correction term must be added. Following Kelly et al.,[12] these two standard states for species X are given by

$$\Delta G*(X(g)) = \Delta G°(X(g)) + \Delta G°^{\rightarrow}* \quad (2)$$

and

$$\Delta G*_{solv}(X) = \Delta G°_{solv}(X) - \Delta G°^{\rightarrow}* \quad (3)$$

where the correction term $\Delta G°^{\rightarrow}*$ is expressed as

$$\Delta G°^{\rightarrow}* = RT\ln(24.46) = 1.89\ \text{kcal/mol}\ (T = 298.15\ \text{K}) \quad (4)$$

$\Delta G°^{\rightarrow}*$ is the free energy change of 1 mole of gas from 1 atm (24.46 L mol^{-1}) to 1 M (1 mol L^{-1}). The $\Delta G°_{aq,\,deprot}(BH^+)$ is given by

$$\Delta G°_{aq,deprot}(BH^+) = \Delta G°(B(aq)) + \Delta G°(H^+(aq)) - \Delta G°(BH^+(aq)) = \Delta G°_{g,deprot}(BH^+) + \Delta G°^{\rightarrow}* + \{\Delta G*_{solv}(B) + \Delta G*_{solv}(H^+) - \Delta G*_{solv}(BH^+)\} \quad (5)$$

2.2. Gas-Phase Calculations. Electronic structure calculations were performed with the *Jaguar 6.5* quantum chemistry software.[9] DFT calculations were carried out using Becke's[13] three-parameter functional and the correlation function of Lee, Yang, and Parr[14] (B3LYP) with a 6-31++G** basis set. In several previous studies of nitrogen-containing heterocyclic compounds, this methodology gave results comparable in accuracy to calculations that employed more extended basis sets[10] (aug-cc-pVXZ, X = D,T) and higher level of theory (G3B3).[15] To assess the effect of basis set size, we also performed full geometry optimizations for **1**−**10** at the B3LYP/aug-cc-pVTZ(-f) level of theory.[16] Frequency calculations, which are generally computationally expensive, were carried out using the 6-31G** basis set. The standard Gibbs free energy of each species (X) in the gas phase is given by

$$\Delta G^{\circ}(\mathrm{X(g)}) = E_{0\mathrm{K}}(\mathrm{X(g)}) + \mathrm{ZPE(X(g))} + \Delta G_{0\rightarrow 298}(\mathrm{X(g)}) \quad (6)$$

where E_{0K} is total electronic energy at 0 K, ZPE is the zero-point vibrational energy, and $\Delta G_{0\rightarrow 298}$ is the Gibbs free energy change from 0 to 298 K at 1 atm calculated using the rigid rotor−harmonic oscillator approximation without scaling. For the standard free energy of the proton, we used $\Delta G^{\circ}(H^+(g)) = 2.5RT - T\Delta S^{\circ} = 1.48 - 7.76 = -6.28$ kcal/mol.[6a,6g]

2.3. Aqueous-Phase Calculations. The coupling of DFT with a Poison−Boltzmann (PB) continuum solvent can provide accurate estimates of the solvation free energies of nitrogen-containing heterocyclic compounds in water.[10] This involves the numerical solution of the PB equation to determine the self-consistent reaction field (SCRF) of the solvent acting on the quantum mechanical solute. In this approach, the solute is described as a low-dielectric cavity ($\epsilon_{solute} = 1.0$) immersed in a continuum solvent characterized by two properties: the solvent probe radius (r_{probe} =1.4 for water) and the solvent dielectric constant ($\epsilon_{solvent} = 80.0$) for water. The dielectric solute/solvent boundary was taken as the solvent-accessible surface area (SASA) defined by the probe radius. The charge distribution of the solute was represented by atom-centered point charges based on electrostatic potential (ESP) fits. The nonelectrostatic component (e.g., cavity term) of the solvation free energy was calculated using the empirical relation given in ref 17. The atomic radii used to determine the van der Wall envelope of the solute were taken from Tannor et al.[17] without modifications[18] (1.9 Å for sp^3-hybridized carbon, 1.6 Å for nitrogen and oxygen, and 1.15 Å for hydrogen). Calculations were carried out using both gas-phase geometries and geometries optimized in the solvent reaction field.

2.4. Proton Free Energy of Solvation [$\Delta G^*_{solv}(H^+)$]. The absolute value of $\Delta G^*_{solv}(H^+)$ is still the subject of ongoing debate in the literature.[19] A recent study of Kelly at al.[12] (based on cluster−pair approximation) yielded a value of $\Delta G^*_{solv}(H^+) = -266.1$ kcal/mol. This agrees very well with the value of −265.9 kcal/ mol reported by Tissandier et al.[19] However, the experimental uncertainty of $\Delta G^*_{solv}(H^+)$ is still ≥2 kcal/mol. In this study, $\Delta G^*_{solv}(H^+)$ was treated as a parameter and its value was adjusted to give the best match between theory and experiment. The selected values of $\Delta G^*_{solv}(H^+)$ were, respectively, equal to −267.9 kcal/mol and −267.6 kcal/mol for calculations using solution-phase and gas-phase optimized geometries. Note that these values fall within the estimated experimental uncertainty of $\Delta G^*_{solv}(H^+)$.

2.5. Conformational Analysis. The protonated and deprotonated forms of **11**−**23** can exist in multiple conformations. Thus, a constrained search was carried out to locate their lowest-energy conformers. Although a full sampling of conformational space was beyond the scope of this study, we identified many of the lowest-energy conformers in the gas phase and solution phase for the neutral and protonated forms of **11**−**23**. pK_a values were computed using the lowest-energy forms in solution.[8]

2.6. Statistical Corrections for Compounds with Multiple Ionizable Groups. Finally, we corrected the calculated pK_a values to account for the presence of multiple ionizable groups in a ligand. Thus, we added the statistical factor log 2 to the first pK_a (pK_{a1}) and subtracted it from the second pK_a (pK_{a2}) for compounds with two identical amino groups, following the work of Perrin et al.[20] and Jang et al.[10c] Note that for ligands with n identical amino groups, the statistical correction for the protonation state i (pK_{ai}) is equal to $\log\{(n - i + 1)/i\}$.[20]

3. Results and Discussion

pK_a calculations for aliphatic amines (**1**−**10**), diamines (**11**−**17**), and aminoamides (**18**−**23**) are discussed in separate sections as given below. In all cases, we carried out a detailed conformational search to locate the relevant lowest-energy conformers. Initially, we tested and calibrated our pK_a computational methodology using aliphatic amines with one or two major conformers. We then applied the same methodology to the more flexible amino compounds.

3.1. Aliphatic Amines. The only relevant conformation for **1** and **5**−**10** is a staggered arrangement of their atoms about the C−N bond as previously reported for methylamine.[21] In contrast, **2**−**4** exhibit a trans and a gauche conformations due to the different orientation of their methyl groups relative to the electron lone pairs of their nitrogen atoms. The relative free energies of the conformers in the gas and aqueous phases are comparable, differing only by 0−0.36 kcal/mol in favor of the trans conformer. These results are consistent with recent FTIR studies of ethylamine in liquid krypton and xenon[22] indicating that its two conformers are populated in significant amounts, with the trans conformer being the most stable.

Table 1 summarizes the calculated and measured values[12,23,24] of the gas-phase proton affinities (PA), basicities (GB), and solvation energies for the neutral and protonated aliphatic amines calculated at the B3LYP/6-31++G** level of theory. Calculated GB values include the entropy contributions due to the rotational symmetry of the molecules. The calculated enthalpy (PA) and Gibbs free energy (GB) changes for deprotonation of the protonated amine species in the gas phase are in excellent agreement with experimental values, with a mean absolute error of 0.7−0.8 kcal/mol. The mean error of the calculated solvation free energies (1.2−1.4 kcal/mol) is higher, especially for secondary and tertiary amines. To the best of our knowledge, no markedly improved results have been reported for these systems using continuum solvent models[18] or explicit solvent models with pairwise-additive[25] and polarizable potentials.[26] Surprisingly, the same overall level of accuracy is achieved for all the protonated species. Thus, no scaling of the van der Wall radii is needed to reproduce the measured free energies of solvation of the alkylamine ions.

We also performed DFT geometry optimization at the B3LYP/aug-cc-pVTZ(-f) level of theory. A detailed comparison of gas-phase and aqueous-phase free energy contributions is given in Table 1S of Supporting Information. The mean absolute errors between calculated and measured gas-phase PA, GB, $\Delta G^*_{solv}(B)$, and $\Delta G^*_{solv}(BH^+)$ are, respectively, equal to 0.41, 0.64, 1.6, and 1.1 kcal/mol. Note that addition of polarization and diffuse functions leads to a slight improvement of the gas-phase results. Conversely, a notable decline in accuracy for the

TABLE 1: Calculated and Measured Gas-Phase Proton Affinities (PA), Basicities (GB), and Solvation Energies of Neutral (B) and Protonated (BH^+) Aliphatic Amines (energies in kcal/mol)

		PA		GB		ΔG^*_{solv} (B)			ΔG^*_{solv} (BH^+)		
	base	calc[a]	expt[d]	calc[a]	expt[d]	no aq opt[b]	aq opt[c]	expt[e]	no aq opt[b]	aq opt[c]	expt[f]
1	methylamine	215.45	214.9	207. 27	206.6	−4.97	−5.03	−4.56	−78.49	−78.7	−76.4
2	ethylamine	218.91	218.0	211. 44	210.0	−4.98	−5.01	−4.50	−74.07	−74.4	
3	propylamine	220.04	219.4	212. 61	211.3	−4.71	−4.68	−4.39	−72.35	−72.6	−71.5
4	isopropylamine	221.56	220.8	214. 10	212.5	−4.45	−4.54		−70.55	−70.9	
5	*tert*-butylamine	224.29	223.3	216. 18	215.1	−4.34	−4.49		−67.25	−67.7	−67.3
6	dimethylamine	222.28	222.2	214. 36	214.3	−2.72	−2.82	−4.29	−69.42	−69.6	−68.6
7	diethylamine	228.23	227.6	220. 36	219.7	−2.15	−2.15	−4.07	−62.26	−62.5	−63.4
8	dipropylamine	230.36	230.0	222. 54	222.1	−1.93	−0.82	−3.66	−59.08	−59.3	−60.5
9	trimethylamine	226.43	226.8	218. 97	219.4	−1.12	−1.22	−3.23	−62.19	−62.3	−61.1
10	triethyalamine	234.75	234.7	227. 09	227.0	−0.02	−0.23		−52.93	−53.3	−54.9
mean absolute error		0.54 ± 2.0[g]		0.78 ± 2.0[g]		1.2	1.4	±0.2[g]	1.1	1.3	±3.0[g]

[a] B3LYP/6-31++G** using ZPE and thermal corrections from B3LYP/6-31G**. [b] Single-point calculations in the aqueous phase on the B3LYP/6-31++G** gas-phase geometries. [c] Geometry reoptimization in the aqueous phase at B3LYP/6-31++G** level. [d] Ref 23. [e] Ref 24. [f] Ref 12. [g] An average uncertainty of experimental data.

TABLE 2: Calculated and Measured pK_a Values of Aliphatic Amines[h]

		method I[a]		method II[b]			
no.	base	no aq opt[c]	aq opt[d]	no aq opt[c]	aq opt[d]	Jaguar pK_a module[e]	expt[f]
1	methylamine	11.04	10.91	11.02	10.91	10.1	10.63
2	ethylamine	10.85	10.84	10.81	10.76	11.1	10.70
3	propylamine	10.64	10.66	10.64	10.65	9.9	10.60
4	isopropylamine	10.61	10.62	10.66	10.60	10.6	10.63
5	*tert*-butylamine	9.80	9.79	9.83	9.81	10.4	10.68
6	dimethylamine	11.24	11.09	10.92	10.81	10.8	10.78
7	diethylamine	10.82	10.78	10.93	10.86	10.8	11.02
8	dipropylamine	10.24	11.00	10.39	10.82	10.6	11.00
9	trimethylamine	10.50	10.30	10.63	10.44	10.2	9.80
10	triethyalamine	10.47	10.40	10.81	10.67	10.5	10.75
mean absolute error		0.39	0.28	0.31	0.24	0.32	±0.10[g]

[a] B3LYP/6-31++G** using ZPE and thermal corrections from B3LYP/6-31G**. [b] B3LYP/aug-cc-pVTZ(-f) using ZPE and thermal corrections from B3LYP/6-31G**. [c] Single-point calculations in the aqueous phase at the same level of theory. [d] Geometry optimization in the aqueous phase at the same level of theory. [e] Ref 9. [f] Ref 20. [g] An average uncertainty of experimental data. [h] Method II that employs a larger basis set gives our best estimate of pK_a values.

solvation free energies of neutral species is observed. We speculate that this may be caused by the use of additional diffuse functions. When diffuse functions with slow-decaying exponential tails are employed, a notable fraction of the solute electron density can be located outside the cavity. This reduces the overall interaction energies between the solute and the solvent-induced cavity surface charges.[27] Rescaling of the solute atomic radii to increase the size of the cavity can offset this effect in some cases.[10]

The pK_a values of aliphatic amines are calculated using eq 5 and the corresponding free energy contributions listed in Table 1 and Table 1S. The calculated pK_a (Table 2) values agree very well with the experimental results[20] in most cases. The mean error for the ten amines is 0.3−0.4 pK_a units. Only the calculated pK_a of *tert*-butylamine shows noticeable deviation from experiment (0.9 pK_a unit). Note that the use of the more extended aug-cc-pVTZ basis set gives only minor improvements in the accuracy of the pK_a calculations. Similarly, geometry reoptimization in aqueous solution has a small-to-modest effect on the calculated pK_a of the monoamines. Table 2 shows that our calculated pK_a values are comparable in accuracy with estimates obtained using the *Jaguar 6.5* pK_a prediction module with its default input settings.[9] Recall that the pK_a module of *Jaguar*[8a,9] uses three empirical parameters to correct the calculated "raw" pK_a for each functional group. We find that these corrections are not needed to obtain accurate pK_a values for amines.

3.2. Aliphatic Diamines. Diamines (**11**−**17**) have a large number of rotational isomers. Most previous computation studies have been limited to the characterization of the conformation of diamines in the gas phase.[28−37] Investigations of the conformational stability of solvated diamines have been mostly limited to 1,2-ethanediamine (**11**).[36−38] In this study, we reexamined the conformational isomerism of **11** and **11H**$^+$ in the gas and solution phases. Building upon the results of the conformational analysis of 1,2-ethanediamine (**11**), we also examined all the possible trans and selected gauche forms of **12**−**17** and **12H**$^+$−**17H**$^+$. This enabled us to locate the relevant and low-energy conformations that were employed in subsequent calculations of the pK_a of these compounds.

3.2.1. Conformational Analysis of 1,2-Ethanediamine (11). Tables 3 and 4 give the relative gas-phase and aqueous-phase electronic and Gibbs free energies of ten unique conformers of 1,2-ethanediamine (**11**) and 3 unique conformers of its protonated species (**11H**$^+$). We use previously adopted notations[29,30] for identifying rotational isomers; where a capital letter refers to a gauche (G) or trans (T) isomer (relative to the NCCN angle) and a small letter (t, g, g′) refers to three possible orientations of each amino group. As shown in Table 3, the two gauche conformers of **11** with intramolecular hydrogen bonds are the most stable forms in the gas phase [see **11(g)** in Figure 4], whereas the trans conformers are about 1 kcal/mol higher in energy. This result is consistent with previous calculations[28−31,34−36] and experimental data from microwave spectroscopy[39] and electron diffraction.[40] However, the conformational behavior of **11** is quite different in the solution phase. We find that the most stable forms in aqueous solution are trans,

TABLE 3: Calculated Relative Energies (kcal/mol) for Ten Conformations[a] of 1,2-Ethanediamine (11) and Their Relative Populations Based on Boltzmann Distribution in the Gas Phase and Aqueous Phase[g]

	gGg′	tGg′	gGg	tGg	tGt	g′Gg′	tTt	tTg	gTg	gTg′
$\Delta E_{0K,rel}$(g)	0.00	0.18	0.56	1.17	1.20	3.70	1.10	1.31	1.42	1.45
ZPE(g)	69.8 3	69.78	69.76	69.58	69.56	69.15	69.56	69.53	69.44	69.50
$\Delta\Delta G_{0\rightarrow 298K}$ (g)	−17. 17	−17.22	−16.9 5	−17.37	−16.8 6	−17.59	−16.92	−17.36	−17.01	−17.42
ΔG°_{rel}(g)	0.00	0.08	0.72	0.72	1.24	2.61	1.07	0.82	1.19	0.87
Population(g)[b]	0.35	0.30	0.05	0.10	0.02	2×10^{-3}	0.01	0.09	0.02	0.04
ΔG^{*}_{solv}	−9.1 9	−9.52	−9.28	−10.20	−10.7 1	*f*	−10.96	−10.91	*f*	−11.37
ΔE^{*}_{rel}(aq)[c]	**0.73**	**0.58**	**1.62**	**0.89**	**0.82**		**0.47**	**0.32**		**0.00**
ΔG^{*}_{rel}(aq) I[d]	1.31	1.06	1.94	1.02	1.03		0.62	0.41		0.00
ZPE(aq)	69.4 0	69.43	69.44	69.52	69.52		69.52	69.57		69.36
$\Delta\Delta G_{0\rightarrow 298K}$ (aq)	−17. 46	−17.43	−17.0 0	−17.34	−17.0 2		−17.03	−17.39		−17.39
ΔG^{*}_{rel}(aq) II[e]	**0.70**	**0.62**	**1.68**	**1.11**	**0.95**		**0.59**	**0.53**		**0.00**
Population(a q) II[b,e]	0.16	0.18	0.02	0.08	0.05		0.05	0.21		0.26

[a] We use previously[29,30] adopted notations for different isomers that are briefly described in section 3.2.1. [b] The calculated population probability takes into account the number of identical conformers. [c] Relative electronic energies in aqueous solution that include rotational symmetry corrections. [d] Relative free energies in aqueous solution calculated using gas-phase ZPE and thermal corrections. [e] Relative free energies in aqueous solution calculated using aqueous-phase ZPE and thermal corrections. [f] Corresponding conformations are not stable in the aqueous phase and convert to other rotational isomers. [g] Numbers in bold illustrate similarity between ΔE^{*}_{rel}(aq) and more computationally expensive ΔG^{*}_{rel}(aq) II that include frequency calculations in the solvent.

TABLE 4: Calculated Relative Energies (kcal/mol) for Conformations[a] of Protonated 1,2-Ethanediamine ($11H^{+}$) and Their Relative Populations Based on Boltzmann Distribution in the Gas Phase and Aqueous Phase[f]

	Gg	Tt	Tg
$\Delta E_{0K,rel}$(g)	0.00	12.09	10.39
ZPE(g)	79.14	78.61	78.64
$\Delta\Delta G_{0\rightarrow 298K}$(g)	−17.02	−17.58	−17.71
ΔG°_{rel}(g)	0.00	11.00	9.19
Population(g)[b]	100	4×10^{-9}	2×10^{-7}
ΔG^{*}_{solv}	−69.29	−81.00	−78.83
ΔE^{*}_{rel}(aq)[c]	**0.00**	**0.38**	**0.85**
ΔG^{*}_{rel}(aq) I[d]	0.71	0.00	0.36
ZPE(aq)	79.08	79.10	79.11
$\Delta\Delta G_{0\rightarrow 298K}$(aq)	−17.70	−17.60	−17.57
ΔG^{*}_{rel}(aq), II[e]	**0.00**	**0.46**	**0.97**
Population(aq) II[b,e]	0.70	0.16	0.14

[a−e] See footnotes to Table 3. [f] Numbers in bold illustrate similarity between ΔE^{*}_{rel}(aq) and more computationally expensive ΔG^{*}_{rel}(aq) II that include frequency calculations in the solvent.

followed by gauche [see **11(aq)** in Figure 4]. These results are consistent with Raman spectroscopic investigations[36] and recent molecular dynamics simulations[38b] (with explicit SPC/E water molecules) of 1,2-ethanediamine in solutions showing a predominant population of the trans conformation. Note that previous MP2/6-31G** calculations on **11** (with inclusion of solvent effects through interactions with the solute dipole moment) did not predict the correct order of stability of its gauche and trans isomers in solution.[36]

The partially protonated 1,2-ethanediamine [see **$11H^{+}$(g)** in Figure 4] predominantly exists in a gauche conformation stabilized by intramolecular N−H^{+}···N hydrogen bonding in agreement with previous gas-phase calculations.[33,34] The two trans conformations were found to be less stable by 9.2 and 11.0 kcal/mol (Table 4). Conversely, all conformers of **$11H^{+}$** in solution are within 1 kcal/mol of each other. We tested three methods of estimation of the free energies of solvation of **$11H^{+}$**. In the first approach [(ΔE^{*}_{rel}(aq)], we added calculated electronic energies in the gas phase to the free energies of solvation that were calculated using solution-phase optimized geometries. In the second approach [(ΔG^{*}_{rel}(aq) I], we corrected [ΔE^{*}_{rel}(aq)] by adding ZPE and thermal corrections to the calculated gas-phase energies. In the third approach [(ΔG^{*}_{rel}(aq) II], we corrected [ΔE^{*}_{rel}(aq)] by adding ZPE and thermal corrections calculated using solution-phase optimized geometries to account for solvent effects on molecular vibrations. Note that calculations of solvation free-energy based on gas-phase frequency corrections lead to the incorrect order of stability for the **$11H^{+}$** conformers. Note also that the ZPE and vibrational contributions to the solvation free energies of the conformers become almost averaged out in solution. This enables us to use method ΔE^{*}_{rel}(aq) to estimate the relative populations of the different **11H** and **$11H^{+}$** conformers and determine the most stable structures in solutions (after taking into consideration their rotational entropy) without performing expensive Hessian calculations in solution.

*3.2.2. Conformational Analysis of Compounds **12**−**17**.* We also located and analyzed most of the relevant conformers of **12**−**17** and **$12H^{+}$**−**$17H^{+}$**. The results are summarized in Figure 4 and Table 5. In the gas phase, the lowest-energy conformer of **12** is similar to **11** and corresponds to a structure with intramolecular hydrogen bonding. In contrast, the most stable form of **13** is the trans conformer. Note that its gauche conformer (with internal hydrogen bond) is only 0.5 kcal/mol higher in energy. These results are consistent with previous electronic structure calculations for **12** and **13**.[29,32,34] Note that the lowest-energy form of **16** adopts one of the gauche conformations stabilized by C−H···N hydrogen bonding [see **16(g)** in Figure 4]. We also found conformers with similar structures for **15** and **17**, although with slightly higher energies (by 0.1−0.3 kcal/mol) than their lowest-energy trans conformers. This result is inconsistent with recent MP2/6-311+G** calculations[35] showing that the C−H···N hydrogen-bonded conformer of **15** is 3.8 kcal/mol more stable than one of its trans isomers. To shed light into this inconsistency, we optimized these two conformers of **15** at the same MP2/6-311+G** level of theory[41] as in ref 35. We found that the relative energies of the conformers differ by less than 0.1 kcal/mol (in favor of the hydrogen-bonded form) thereby suggesting that the most stable trans form of **15** was not previously located.

Conformational flexibility of protonated diamines in the gas phase is severely restricted due to formation of intramolecular hydrogen bonds [see **$11H^{+}$(g)**−**$17H^{+}$(g)** in Figure 4]. The strength of this interaction can be roughly estimated by the difference in energy between the hydrogen-bonded conformer and the most stable trans conformer (Table 5). It can also be characterized by the H···N contact distance and N−H···N angle (Table 6). Consistent with previous analysis for **$11H^{+}$**−**$13H^{+}$**,[33,34] the internal hydrogen bond becomes stronger upon increasing the spacing between the two amino groups from two

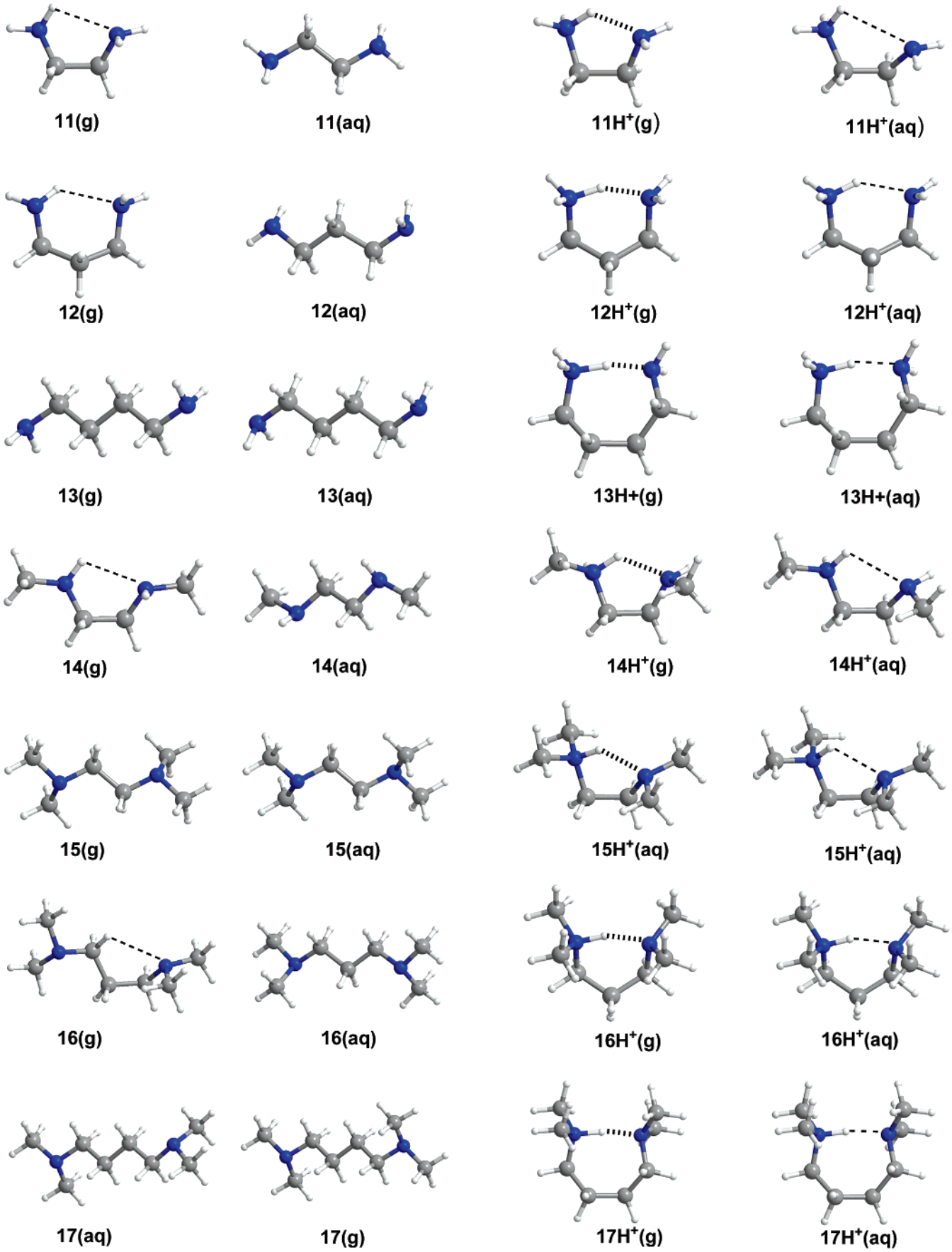

Figure 4. Lowest-energy structures of neutral and protonated alkyldiamines in the gas phase and aqueous solution.

to four carbon atoms. Conversely, it becomes weaker with the replacement of the two amino hydrogen atoms by methyl groups. A similar trend has been observed for the electronic binding energies of complexes of protonated amines with neutral

TABLE 5: Calculated[a] Relative Energies (kcal/mol) for the Most Stable[b] Trans and Gauche Conformers of 11−17 and 11H$^+$−17H$^+$

		neutral,[c]	protonated	
no.	base	gas phase	gas phase	aq phase
11	1,2-ethanediamine	1.10	10.39	0.41
12	1,3-propanediamine	1.13	16.23	0.42
13	1,4-butanediamine	−0.53	20.02	1.41
14	*N*,*N*′-dimethyl-1,2-ethanediamine	1.58	9.33	0.61
15	*N*,*N*,*N*′,*N*′-tetramethyl-1,2-ethanediamine	−0.28	8.98	1.20
16	*N*,*N*,*N*′,*N*′-tetramethyl-1,3-propanediamine	0.18	13.44	1.81
17	*N*,*N*,*N*′,*N*′-tetramethyl-1,4-butanediamine	−0.13	15.71	2.53

[a] The structures of the most stable conformers are shown in Figure 4. [b] The plus (minus) sign indicates that the lowest-energy form adopts a gauche (trans) configuration. [c] The relative energies of the less stable gauche conformers of **11**−**17** in aqueous environment are not shown because the exhaustive conformational search of higher-energy isomers was not performed.

TABLE 6: Geometric Parameters of Neutral and Protonated Aliphatic Diamines That Possess Intramolecular Hydrogen Bonds[a]

	neutral, gas phase		protonated			
			gas phase		aq phase	
no.	H···N	N−H···N	N···H	N−H···N	N···H	N−H···N
11	2.509	103.5	1.878	123.5	2.738	97.5
12	2.295	125.1	1.645	150.5	1.973	139.9
13	2.106	148.5	1.543	165.8	1.717	161.6
14	2.498	105.9	1.931	123.5	2.460	107.1
15			1.930	125.7	2.318	113.5
16			1.702	154.3	1.810	151.2
17			1.611	171.0	1.700	169.3

[a] Bond lengths in Å, angles in deg.

amines.[42] In the aqueous phase, the lowest-energy forms of the neutral diamines [see **11(aq)**−**17(aq)** in Figure 4] are structurally similar and correspond to all-trans conformations. These structures are better exposed to the solvent and thus have higher solvation energies. Conversely, the most stable conformers for the protonated diamines [see **11H$^+$(aq)**−**17H$^+$ (aq)** in Figure 4] maintain their hydrogen-bonded conformations in solution. However, the hydrogen-bonding interactions are significantly weaker in this case, as shown in Tables 5 and 6.

3.2.3. pK_a *Prediction for Alkyldiamines.* Table 7 lists the gas-phase deprotonation free energies for the partially (BH^+) and fully protonated (BH_2^{2+}) diamines and their solvation free energies. These were calculated using the lowest-energy conformers in the aqueous solution. Table 7 shows that geometry optimization in solution is critical for partially protonated diamine systems with intramolecular hydrogen bonds but has a smaller effect on the neutral and fully protonated diamines with all-trans conformations. The calculated pK_a values of **11**−**17** are listed in Table 8. Note the excellent agreement between the calculated and measured[43] pK_a values when geometry optimization in the solvent is carried out. For six of the alkyldiamines evaluated in this study, the mean absolute error between calculations for the first pK_a (pK_{a1}) is ∼0.3 pK_a units. The largest deviation is ∼0.7 pK_a units. Conversely, the mean absolute error increases to ∼0.7 pK_a units (with the largest deviation ∼1.2 pK_a units) when gas-phase optimized structures are employed in the pK_a calculations. Note that these calculations reproduce the observed increase in the pK_a of alkyldiamines with longer alkyl chains and replacement of amino hydrogen atoms with methyl groups.

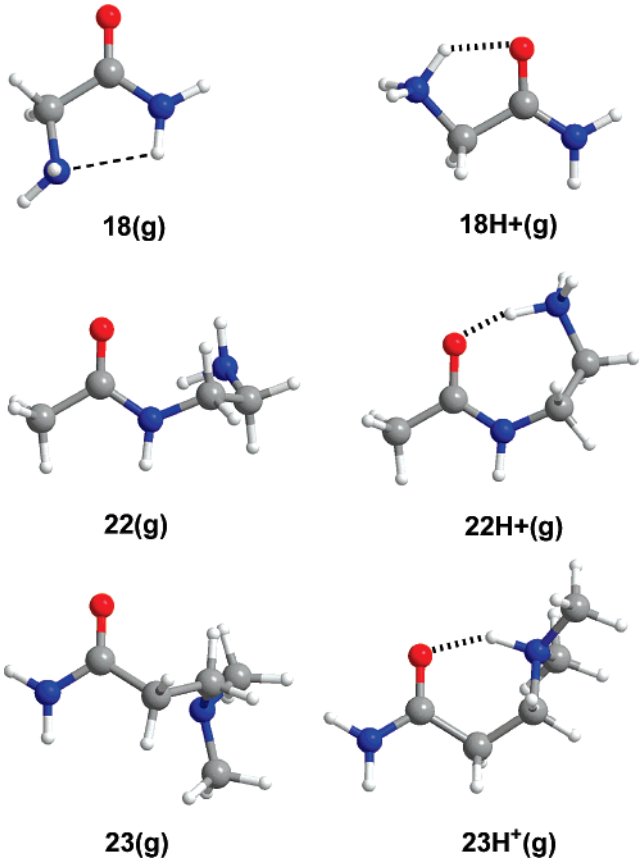

Figure 5. Lowest-energy structures of selected neutral and protonated aminoamides in the gas phase.

As shown in Table 8, the second acidity constants (pK_{a2}) of **11**−**17** are also in excellent agreement with experimental measurements when the calculations are carried out using solution-phase optimized structures. Note that the calculations of pK_{a2} values are of accuracy comparable with those of pK_{a1} values. This result is surprising given the fact that calculations involving ions with multiple charges and/ or high charge-to-volume ratios tend to be less accurate unless explicit water molecules are added to the solute to account for specific interactions. However, as shown by Pliego and co-workers,[44] the effect of explicit water molecules on calculated solvation energies of ammonium and alkylammonium ions is relatively small. Thus, one can obtain reasonably good results without using explicit water in this case.

3.3. Aminoamides. Aminoamides (**18**−**23**) can act as both proton donors and proton acceptors and form intramolecular hydrogen bonds. The most stable forms of the neutral and protonated species of 2-aminoacetamide (**18**) are depicted in Figure 5. Similar structures with N−H···N and N−H$^+$···O hydrogen bonds are also found for the neutral and protonated species of **19**−**21**. In contrast, **22** and **23** only exhibit intramolecular hydrogen-bonding interactions in the protonated state (Figure 5). The solvent does not change the most stable gas-phase hydrogen-bonded conformations of neutral and protonated aminoamides.

Table 9 highlights the effects of solute−solvent interactions on the geometric parameters of the hydrogen-bonded conformations. Note that replacing the amide hydrogen atoms with methyl groups reduces the length of the N−H$^+$···O hydrogen bond. Conversely, this bond increases when the amine hydrogen atoms

TABLE 7: Calculated Free Energy Contributions[a] (kcal/mol) to pK_a Values for 11−17 and 11H$^+$−17H$^+$

no.	$\Delta G°_{g,deprot}$ (BH^+)	$\Delta G°_{g,deprot}$ (BH_2^{2+})	ΔG^*_{solv} (B)		ΔG^*_{solv} (BH^+)		ΔG^*_{solv} (BH_2^{2+})	
			no aq opt	aq opt	no aq opt	aq opt	no aq opt	aq opt
11	221.17	104.57	−11.09	−11.37	−67.0	−69.3	−240.1	−240.8
12	228.09	119.37	−10.95	−10.77	−61.6	−62.6	−222.1	−222.8
13	232.36	130.06	−11.46	−11.26	−58.6	−59.3	−208.4	−208.8
14	227.15	120.51	−6.13	−6.43	−57.6	−58.9	−213.9	−214.9
15	231.25	130.04	−3.37	−3.43	−50.5	−51.2	−194.4	−195.1
16	235.37	141.35	−3.09	−3.25	−47.6	−47.5	−182.5	−182.9
17	237.31	151.99	−2.91	−3.12	−45.8	−45.9	−172.1	−172.7

[a] Calculated thermodynamic data correspond to the lowest-energy acid/base pair in aqueous solution.

TABLE 8: Calculated and Experimental First and Second pK_a Values of Aliphatic Diamines, 11−17

no.	pK_{a1}			pK_{a2}		
	no aq opt	aq opt	expt[a]	no aq opt	aq opt	expt[a]
11	8.66	9.89	9.9−10.2	8.44	7.10	6.8−7.5
12	9.83	10.52	10.1−10.7	10.10	9.59	8.3−9.0
13	10.40	10.82	10.7−10.8	10.04	9.69	9.0−9.6
14	9.79	10.25	9.9−10.3	7.80	7.44	6.8−7.5
15	9.60	9.81	9.0−9.2	5.70	5.55	5.6−5.9
16	10.65	10.31	9.7−9.8	7.47	7.54	7.5−7.7
17	10.94	10.66		8.93	9.04	

[a] A range of experimental pK_a values is shown to estimate the accuracy of experimental data compiled in ref 43; the estimated uncertainty is ±0.1−0.3 pK_a units.

are replaced by methyl groups. These results are consistent with the electronic effect of the methyl group. For **22H**$^+$, hydrogen-bonding provides the strongest stabilization. In this case, six heavy atoms form a cyclic conformation that allows almost a linear arrangement of the three atoms in the N−H$^+$···O bond.

The calculated pK_a and relevant thermodynamic data for **18**−**23** are presented in Table 10. The calculated deprotonation free energies in the gas phase increase with the number of methyl groups bonded to the amine or amide group. Conversely, the solvation free energies for **18**−**21** and **18H**$^+$−**21H**$^+$ follow the opposite trend as observed for mono- and diamines. Interestingly, the calculated pK_a values do not exactly follow either of those trends. Here again, we would like to emphasize the critical role of solution-phase geometry optimization for accurate prediction of pK_a values. Table 10 shows excellent agreement (within 0.3 pK_a units) between the calculated and experimental pK_a of the amidoamines when they are optimized in solution. Conversely, the mean deviation between the calculated and measured pK_a increases by a factor of 4 when the aminoamides are optimized in the gas phase.

4. Conclusions

In this article, we couple density functional theory with a Poisson−Boltzmann continuum solvent model to calculate the acidity constants (pK_a) of aliphatic amines, diamines, and aminoamides in aqueous solutions. These compounds are building blocks for several classes of dendrimers. The calculation protocol is grounded in a well-defined computational framework with only one adjustable parameter: the free energy of solvation of the proton (H^+). No empirical correction terms were employed in the calculations. A key step in the pK_a calculations was to locate the relevant low-energy conformers. Conformational analysis of 1,2-ethanediamine suggested that the relative populations of different isomers in the aqueous phase can be determined from the relative electronic energies, ΔE^*_{rel}(aq), without performing time-consuming Hessian calculations in solution. The results establish that the lowest-energy conformations for neutral alkyldiamines in the gas phase are not generally the most stable structures in aqueous solution, in agreement with recent MD simulations in explicit solvent and experimental data for 1,2-ethanediamine. However, even if the intramolecular hydrogen bond is maintained in solution, such

TABLE 9: Geometric Parameters of Neutral and Protonated Aminoamides That Possess Intramolecular Hydrogen Bonds[a]

no.[b]	neutral				protonated			
	gas phase		aq phase		gas phase		aq phase	
	H···N	N−H···N	H···N	N−H···N	H···O	N−H···O	H···O	N−H···O
18	2.247	106.2	2.396	102.1	1.707	126.2	2.050	114.5
19	2.272	105.7	2.372	102.6	1.769	125.0	2.271	101.9
20	2.205	110.0	2.333	105.6	1.736	126.3	2.252	103.4
21					1.671	128.4	2.162	104.4
22					1.471	163.0	1.855	148.1
23					1.683	146.5	1.964	133.8

[a] Bond lengths in Å, angles in deg. [b] Chemical names and formulas of **18**−**23** are given in Figure 2 and Table 10.

TABLE 10: Calculated Free Energy Contributions[a] (kcal/mol) and pK_a Values of Aminoamides, 18−23

no.	base	$\Delta G_g°$(B H$^+$)	ΔG^*_{solv} (B)		ΔG^*_{solv} (BH^+)		pK_a		
			no aq opt	aq opt	no aq opt	aq opt	no aq opt	aq opt	expt[b]
18	2-aminoacetamide	210.56	−13.93	−14.64	−78.19	−80.63	6.67	7.73	7.95
19	2-methylaminoacetamide	217.48	−12.12	−12.70	−70.67	−72.74	7.56	8.43	8.31
20	*N*-methyl-2-methylaminoacetamide	219.73	−9.66	−10.68	−65.49	−68.17	7.21	8.23	8.24
21	*N*,*N*-dimethyl-2-methylaminoacetamide	225.22	−9.45	−10.42	−61.38	−63.46	8.37	8.98	8.82
22	*N*-(2-aminoethyl)acetamide	225.34	−15.09	−14.66	−65.44	−68.27	7.31	9.49	9.25
23	3-dimethylaminopropionamide	231.27	−12.55	−13.38	−58.94	−59.97	8.75	8.69	

[a] Calculated thermodynamic data corresponds to the lowest-energy acid/base pair in aqueous solution. [b] Ref 43: an average uncertainty of experimental data is ± 0.1 pK_a units.

as in **18**−**21** and **11H**$^+$−**23H**$^+$, geometry changes upon solvation are usually significant and subsequent changes in solvation energies are not negligible.

The use of solution-phase optimized geometries gives calculated pK_a values in excellent agreement with experimental measurements. The mean absolute error is <0.5 pK_a unit in all cases. Conversely, calculations for diamines and aminoamides based on gas-phase geometries lead to a mean absolute error >0.5 pK_a unit compared to experimental measurements. We find that geometry optimization in solution is essential for making accurate pK_a predictions for systems possessing intramolecular hydrogen bonds.

Acknowledgment. This work was carried out in the Materials Process Simulation Center of the Division of Chemistry and Chemical Engineering at the California Institute of Technology. Funding for this work was provided by the National Science Foundation (NIRT CBET Award No. 0506951). Supplemental funding for this research was provided by the U.S. Environmental Protection Agency (STAR Grant RD-83252501). The computational facilities used in these studies were funded by grants from ARO-DURIP, ONR-DURIP, and NSF-MRI. All DFT calculations were carried out using the *Jaguar 6.5* quantum chemistry software.

Supporting Information Available: Cartesian coordinates and energies (Hartrees) for the lowest-energy forms of the studied neutral and protonated aliphatic diamines and aminoamides obtained at the B3LYP/6-31++G** level with and without the effect of the solvent, and a table comparing calculated (B3LYP/aug-cc-pVTZ(-f)) and experimental gas-phase proton affinities, basicities, and solvation free energies of aliphatic amines. This material is available free of charge via the Internet at http://pubs.acs.org.

References and Notes

(1) Lehninger, A. L.; Nelson, D. L.; Cox, M. M. *Principles of Biochemistry*, 2nd ed.; Worth Publishers: New York, 1993.

(2) (a) Steed, J.; Atwood, J. *Supramolecular Chemistry*; John Wiley and Sons, LTD: Chichester, 2000. (b) Schneider, H.-J.; Yatsimirsky, A. *Principles and Methods in Supramolecular Chemistry*; John Wiley and Sons, LTD: Chichester, 2000.

(3) (a) Gale, P. A. *Coord. Chem. Rev.* **2000**, *199*, 181. (b) Gale, P. A. *Coord. Chem. Rev.* **2001**, *213*, 79. (c) Fitzmaurice, R. J.; Kyne, G. M.; Douheret, D.; Kilburn, J. D. *J. Chem. Soc., Perkin Trans. 1* **2002**, 841.

(4) (a) Sigel, H.; Martin, R. B. *Chem. Rev.* **1982**, *82*, 385. (b) Clement, O.; Rapko, B. M.; Hay, B. P. *Coord. Chem. Rev.* **1998**, *170*, 230.

(5) *Dendrimers and other Dendritic Polymers*; Fréchet, J. M. J., Tomalia, D. A., Eds.; Wiley and Sons: New York, 2001.

(6) (a) Lim, C; Bashford, D.; Karplus, M. *J. Phys. Chem.* **1991**, *95*, 5610. (b) Tunon, I.; Silla, E.; Tomasi, J. *J. Phys. Chem.* **1992**, *96*, 9043. (c) Wiberg, K. B.; Castejon, H.; Keith, T. A. *J. Comput. Chem.* **1996**, *17*, 185. (d) Kallies, B.; Mitzner, R. *J. Phys. Chem. B* **1997**, *101*, 2959. (e) Topol, I. A.; Tawa, G. J.; Caldwell, R. A.; Eissenstat, M. A.; Burt, S. K. *J. Phys. Chem. A* **2000**, *104*, 9619. (f) Silva, C. O.; da Silva, E. C.; Nascimento, M. A. C. *J. Phys. Chem. A* **2000**, *104*, 2402. (g) Liptak, M. D.; Shields, G. C. *J. Am. Chem. Soc.* **2001**, *123*, 7314. (h) Liptak, M. D.; Gross, K. C.; Seybold, P. G.; Feldgus, S.; Shields, G. C. *J. Am. Chem. Soc.* **2002**, *124*, 6421. (i) Klamt, A.; Eckert, F.; Diedenhofen, M.; Beck, M. E. *J. Phys. Chem. A* **2003**, *107*, 9380. (j) Camaioni, D. M.; Dupuis, M.; Bentley, J. *J. Phys. Chem. A* **2003**, *107*, 5778. (k) Magill, A. M.; Cavell, K. J.; Yates, B. F. *J. Am. Chem. Soc.* **2004**, *126*, 8717.

(7) (a) Pliego, J. R.; Riveros, J. M. *J. Phys. Chem. A* **2002**, *106*, 7434. (b) Kelly, C. P.; Cramer, C. J.; Truhlar, D. G. *J. Phys. Chem. A* **2006**, *110*, 2493.

(8) (a) Klicic, J.; Friesner, R. A.; Liu, S.-Y.; Guida, W. C. *J. Phys. Chem. A* **2002**, *106*, 1327. (b) Ulander, J.; Broo, A. *Int. J. Quantum Chem.* **2005**, *105*, 866.

(9) (a) *Jaguar, version 6.5*; Schrödinger, LLC: New York, 2006. (b) *Jaguar, version 6.5*, User Manual.

(10) (a) Jang, Y. H.; Sowers, L. C.; Cagin, T.; Goddard, W. A., III. *J. Phys. Chem. A* **2001**, *105*, 274. (b) Rogstad, K. N.; Jang, Y. H.; Sowers, L. C.; Goddard, W. A., III. *Chem Res. Toxicol.* **2003**, *16*, 1455. (c) Jang, Y. H.; Goddard, W. A., III; Noyes, K. T.; Sowers, L. C.; Hwang, S.; Chung, D. S. *J. Phys. Chem. A* **2003**, *107*, 344−357. (d) Hwang, S.; Jang, Y. H.; Chung, D. S. *Bull. Korean Chem. Soc.* **2005**, *26*, 585.

(11) Ben-Naim, A. *Solvation Thermodynamics*; Plenum: New York, 1987.

(12) Kelly, C. P.; Cramer, C. J.; Truhlar, D. G. *J. Phys. Chem. B* **2006**, *110*, 16066.

(13) Becke, A. D. *Phys. Rev. A* **1988**, *38*, 3098.

(14) Lee, C. T.; Yang, W. T.; Parr, R. G. *Phys. Rev. B* **1988**, *37*, 785.

(15) Rao, J. S.; Sastry, G. N. *Int. J. Quantum Chem.* **2006**, *106*, 1217.

(16) (a) Dunning, T. H., Jr. *J. Chem. Phys.* **1989**, *90*, 1007. (b) Kendall, R. A.; Dunning, T. H., Jr.; Harrison, R. J. *J. Chem. Phys.* **1992**, *96*, 6796.

(17) Tannor, D. J.; Marten, B.; Murphy, R.; Friesner, R. A.; Sitkoff, D.; Nicholls, A.; Ringnalda, M.; Goddard, W. A., III; Honig, B. *J. Am. Chem. Soc.* **1994**, *116*, 11875.

(18) Marten, B.; Kim, K.; Cortis, C.; Friesner, A.; Murphy, R. B.; Ringnalda, M. N.; Sitkoff, D.; Honig, B. *J. Phys. Chem.* **1996**, *100*, 11775.

(19) (a) Tissandier, M. D.; Cowen, K. A.; Feng, W. Y.; Gundlach, E.; Cohen, M.; Earhart, A. D.; Coe, J. V. *J. Phys. Chem. A* **1998**, *102*, 7787. (b) Palascak, M. W.; Shields, G. C. *J. Phys. Chem. A* **2004**, *108*, 3692. (c) Camaioni, D. M.; Schwerdtfeger, C. A. *J. Phys. Chem. A* **2005**, *109*, 10795.

(20) Perrin, D. D.; Dempsey, B.; Sergeant, E. P. *pK$_a$ Prediction for Organic Acids and Bases*; Chapman and Hall: New York, 1981.

(21) Lee, S. J.; Mhin, B. J.; Cho, S. J.; Lee, J. Y.; Kim, K. S. *J. Phys. Chem.* **1994**, *98*, 1129.

(22) Durig, J. R.; Zheng, C.; Gounev, T. K.; Herrebout, W. A.; van der Veken, B. J. *J. Phys. Chem.* A **2006**, *110*, 5674.

(23) Lias, S. G.; Bartness, J. E.; Liebman, J. F.; Holmes, J. L.; Levin, R. D.; Mallard, W. G. Ion Energetic Data. In *NIST Chemistry WebBook, NIST Standard Reference Database Number 69*; Linstorm, P. J., Mallard, W. G., Eds.; National Institute of Standards and Technology: Gaithersburg, MD, March 2003.

(24) Kelly, C. P.; Cramer, C. J.; Truhlar, D. G. *J. Chem. Theory Comput.* **2005**, *1*, 1133−1152.

(25) Morgantini, P.-Y.; Kollman, P. A. *J. Am. Chem. Soc.* **1995**, *117*, 6057.

(26) (a) Ding, Y.; Bernardo, D. N.; Krogh-Jespersen, K.; Levy, R. M. *J. Phys. Chem.* **1995**, *99*, 11575. (b) Meng, E. C.; Caldwell, J. W.; Kollman, P. A. *J. Phys. Chem.* **1996**, *100*, 2367.

(27) Barone, V.; Cossi, M. *J. Phys. Chem. A* **1998**, *102*, 1995.

(28) Carballeira, L.; Mosquera, R. A.; Rious, M. A.; Tovar, C. A. *J. Mol. Struct.* **1989**, *193*, 263.

(29) Bultinck, P.; Goeminne, A.; Van de Vondel, D. *J. Mol. Struct. (THEOCHEM)* **1995**, *339*, 1.

(30) Chang, Y.-P.; Su, T.-M.; Li, T.-W.; Chao, I. *J. Phys. Chem. A* **1997**, *101*, 6107.

(31) Kudoh, S.; Takayanagi, M.; Nakata, M.; Ishibashi, T.; Tasumi, M. *J. Mol. Struct.* **1999**, *479*, 41.

(32) Wang, Z.; Chu, I. K.; Rodriquez, C. F.; Hopkinson, A. C.; Siu, K. W. M. *J. Phys. Chem. A* **1999**, *103*, 8700.

(33) Kumar, M. K.; Rao, J. S.; Vairamani, M.; Sastry, G. N. *Chem. Commun.* **2005**, 1420.

(34) Bouchoux, G.; Choret, N.; Berruyer-Penaud, F. *J. Phys. Chem. A* **2001**, *105*, 3989.

(35) Wang, X.; Yang, D.-S. *J. Phys. Chem. A* **2006**, *110*, 7568.

(36) Batista de Carvalho, L. A. E.; Lourenco, L. E.; Marques, M. P. M. *J. Mol. Struct.* **1999**, *482*−*483*, 639.

(37) Boudon, S.; Wipff, G. *J. Mol. Struct. (THEOCHEM)* **1991**, *228*, 61.

(38) (a) Gubskaya, A. V.; Kusalik, P. G. *J. Phys. Chem. A* **2004**, *108*, 7151. (b) Gubskaya, A. V.; Kusalik, P. G. *J. Phys. Chem. A* **2004**, *108*, 7165.

(39) Marstokk, K. M.; Mollendal, H. *J. Mol. Struct.* **1978**, *49*, 221.

(40) Kazerouni, M. R.; Hedberg, L.; Hedberg, K. *J. Am. Chem. Soc.* **1994**, *116*, 5279.

(41) Geometries were optimized at the MP2/6-311+G** level, using GAMESS program. Schmidt, M. W.; Baldridge, K. K.; Boatz, J. A.; Elbert, S. T.; Gordon, M. S.; Jensen, J. H.; Koseki, S.; Matsunaga, N.; Nguyen, K. A.; Su, S. J.; Windus, T. L.; Dupuis, M.; Montgomery, J. A. *J. Comput. Chem.* **1993**, *14*, 1347.

(42) Sorensen, J. B.; Lewin, A. H.; Bowen, J. P. *J. Org. Chem.* **2001**, *66*, 4105.

(43) (a) Perrin, D. D. *Dissociation Constants of Organic Bases in Aqueous Solution*; Butterworths: London, 1965. (b) Perrin, D. D. *Dissociation Constants of Organic Bases in Aqueous Solution, Supplement, 1972*; Butterworths: London, 1972.

(44) Pliego, J. R., Jr.; Riveros, J. M. *J. Phys. Chem. A* **2001**, *105*, 7241.